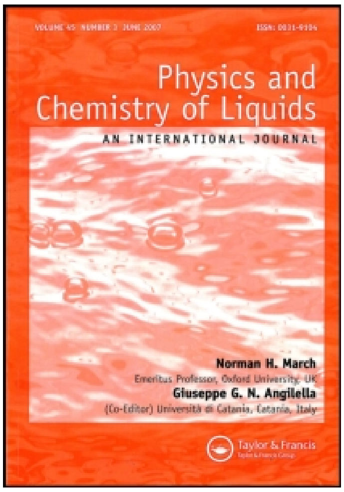

Physics and Chemistry of Liquids
Publication details, including instructions for authors and subscription information:
http://www.informaworld.com/smpp/title~content=t713646857

Structural Parameters of Inert Liquids Part II. Liquid Argon

S. N. Bagchi[a]; J. P. Supple[b]
[a] Physics Department, Concordia University, Montreal, Canada [b] Computel Systems Ltd., Ottawa, Canada

To cite this Article Bagchi, S. N. and Supple, J. P.(1981) 'Structural Parameters of Inert Liquids Part II. Liquid Argon', Physics and Chemistry of Liquids, 11: 1, 1 — 24
To link to this Article: DOI: 10.1080/00319108108079093
URL: http://dx.doi.org/10.1080/00319108108079093

Phys. Chem. Liq., 1981, Vol. 11, pp. 1–24
0031-9104/81/1101–0001$06.50/0

Structural Parameters of Inert Liquids Part II. Liquid Argon

S. N. BAGCHI
Physics Department, Concordia University, Montreal, Canada.

and

J. P. SUPPLE
Computel Systems Ltd., Ottawa, Canada.

(*Received in final form: January 19, 1981*)

The published data on the radial distribution functions (RDF) of liquid argon at various temperatures and pressures have been analyzed on the basis of the Unified Kinematic Theory of Diffraction (see Hosemann & Bagchi),[1] by the method developed before (Bagchi).[2,3] The neighbour statistics, their coordination numbers and other useful relevant structural parameters have been given in the tables. The experimentally obtained RDF curves are compared with the theoretical curves. These figures also show the neighbour statistics. For comparison, one sample of argon vapour near the saturated vapour curve is also analyzed in the same way.

I INTRODUCTION

In previous publications,[3,4] radial distribution functions, $4\pi r^2 g(r)$, of inert liquids and of some simple liquid metals near their melting points as well as of solid copper just below its melting point obtained by various authors from X-ray and neutron diffraction studies have been analyzed by the method developed by one of the authors (see Ref. 2), on the basis of the unified kinematic theory of diffraction (see Ref. 1).

All the RDF curves reported in the literature had been obtained from the inverse transform, Eq. (2), of the intensity function, Eq. (1), derived first by

Zernike & Prins.[5]

$$\bar{I}(u) = \bar{N}(V)\cdot\left[\overline{|\bar{f}_0|^2} + \overline{|\bar{f}_0|^2|D_0|^2}\cdot\frac{2}{u}\int_0^\infty rg_0(r)\sin(2\pi ur)\mathrm{d}r\right] \tag{1}$$

$$4\pi r^2g(r) = 4\pi r^2\bar{\rho} + 8\pi r\int_0^\infty u\cdot i(u)\sin(2\pi ur)\,\mathrm{d}u \tag{2}$$

Here $u(=|\mathbf{b}| = 2\sin\theta/\lambda)$ is the magnitude of the reciprocal distance vector $\mathbf{b}$ and r is the distance vector $|\mathbf{x}|$. $\bar{I}$ is the average intensity function,

$$i(u) = \frac{\bar{I}(u) - \bar{N}\overline{|\bar{f}_0|^2}}{\bar{N}\overline{|\bar{f}_0|^2}} \tag{3}$$

and

$$g(r) = g_0(r) + \bar{\rho} = \bar{\rho}\bar{n}_2(r) \tag{4}$$

$\bar{n}_2(r)$ is the space-time average of the so-called pair-distribution function $n_2(r)$; $\bar{N}(V)$ is the average number of atoms (or molecules) in the volume V and $\bar{\rho}$ is the average macroscopic density. $|f_0|^2$ is the structure factor, $|D_0|^2$ denotes the Debye–Waller factor due to harmonic thermal vibrations of atoms. The symbol $\overline{}$ means that the corresponding function is averaged over all directions of space.

It was assumed that the published data on RDF had been obtained by taking necessary precautions and correcting adequately the observed scattered intensity to get the intensity function $I(u)$ and in calculating its inverse transformation. Thus taking for granted that the function $g(r)$ is accurate enough we have analyzed this function properly in order to get reliable structural parameters, adequate enough to describe the space-time averaged atomic distributions of the liquid state.

For a theoretically correct analysis of $g(r)$ one must first be aware of the inherent limitations of the Eq. (1) and of the physical meaning of $g(r)$. But this would be possible only when we have the most comprehensive kinematic theory of diffraction which degenerates under special circumstances to *all* the conventional theories like Laue–Bragg–Debye–Waller theory for crystals, Zernike–Prins–Debye–Menke theory for liquids and the theories for gases and for amorphous matter developed by Debye, Warren, Guinier and others. The principal aim of the Unified Kinematic Theory[1] was to develop such a theory. This theory not only achieved this goal but also revealed the connections between them and their domains of validity. Moreover, it achieved something more. It explained the diffraction diagrams of matter which cannot be classified so rigidly. In fact, this theory gives the expression for the intensity function for matter of *any kind* on the basis of a single fundamental concept, namely, that of *generalized* lattice. Optical diffraction patterns of many carefully prepared models, whose structural parameters were known previously, quantitatively verified the conclusions derived from this *single* unified theory (see Ref. 1).

In order to realize the significance of the structural parameters of the liquids reported in this series of papers and to understand how they were derived theoretically from the $g(r)$-function, it would be necessary to mention here briefly the basic ideas of this unified theory. For a short exposition of this theory and to know how it led to the method used in this series of papers one should look to the Ref 2. The details of the *actual* evaluation of these parameters were reported in the paper.[3]

II OUTLINE OF THE UNIFIED KINEMATIC THEORY OF DIFFRACTION

For *any* substance the intensity function $I(\mathbf{b})$ and its inverse transform $Q(\mathbf{x})$ are given by, in "Kinematic Theory," (cf. also Refs. 6–9),

$$\left.\begin{aligned} I(\mathbf{b}) &= \mathscr{F}\rho(\mathbf{x})\cdot\mathscr{F}\rho(-\mathbf{x}) \\ Q(\mathbf{x}) = \mathscr{F}^{-1}I(\mathbf{b}) = \rho(\mathbf{x})*\rho(-\mathbf{x}) &= \int\rho(\mathbf{y})\rho(\mathbf{x}+\mathbf{y})\mathrm{d}v_y \end{aligned}\right\} \tag{5}$$

The symbols $\mathscr{F}$, $\mathscr{F}^{-1}$ represent Fourier transformation and its inverse. $*$ represents the symbol of convolution product. $Q(\mathbf{x})$ is denoted as the convolution square of the density function $\rho(\mathbf{x})$. Although Eq. (5) is exact, it does not become useful unless one can express ρ in a convenient form.

In order to describe mathematically the density distribution of *any* substance conveniently one must generalize the concept of the ideal lattice and shall have to distinguish between a lattice and aggregates of lattices which may form again a macro-lattice in which the building blocks are the micro-lattices themselves. The fact that any substance is finite can also be conveniently expressed in terms of the lattice by introducing the shape (or stencil) function $s(\mathbf{x})$ of Ewald.

We define a *generalized lattice* as an indefinitely extended point-structure of weight unity with the origin at $\mathbf{x} = 0$ by

$$z_k = \sum_{k=-\infty}^{\infty} \delta(\mathbf{x} - \mathbf{x}_k) \tag{6}$$

which satisfies the following three conditions.

a) $$\frac{\Delta^2 v}{v} = \frac{\Delta^2 N(V)}{N(V)} = \text{constant for all values of } V \tag{6a}$$

v is the volume of the lattice cell obtained by joining the lattice point located at $\mathbf{x}_k$ with its immediate neighbours by *nonintersecting* vectors.

b) $$\Delta^2 V = N\Delta^2 v, (N \gg 1) \tag{6b}$$

This means that the volume of any lattice cell fluctuates independently.

c) There is no correlation between cell volumes. The lattice cell themselves, however, are arbitrarily distorted and the shape and size of a lattice cell varies in general from one lattice cell to the other quite arbitrarily. One can therefore describe this generalised lattice, which is now statistically homogeneous, with the help of only one normalized *a priori* statistics of the cell volumes, $H(v) \equiv H_{p1p2p3}(\mathbf{x})$. The intensity function of a structure forming a generalized lattice is given by, (see Eq. (50) of Ref. 2),

$$\bar{I}(\mathbf{b}) = \bar{N}(V)[\overline{|f_0|^2} - |D_0|^2|\bar{f}_0|^2] + \frac{1}{\bar{v}}|D_0|^2|\bar{f}_0|^2 Z * |S|^2 \tag{7}$$

where

$$\left.\begin{aligned} z(\mathbf{x}) &= \lim_{M\to\infty}\frac{1}{M}\sum_{m=1}^{\pm M}\sum_{k=1}^{\pm M}\delta(\mathbf{x}-\mathbf{x}_m+x_k) \\ S(\mathbf{b}) &= \mathscr{F}s(\mathbf{x});\ D_0(\mathbf{b}) = \mathscr{F}A_0(\mathbf{x});\ Z(\mathbf{b}) = \mathscr{F}z(\mathbf{x}) \\ A_0(\mathbf{x}) &= \overline{A_p(\mathbf{x})} = \overline{\delta(x-\Delta\mathbf{x}_p)} \\ \bar{\rho}(\mathbf{x}) &= \bar{\rho}_0 * [z(\mathbf{x}) * \delta(\mathbf{x}-\Delta\mathbf{x}_p)]\cdot s(\mathbf{x}) \end{aligned}\right\} \tag{8}$$

$|S|^2$ is called the shape factor. $\delta(\mathbf{x})$ is Dirac's delta function.

The distinctive and characteristic features of the diffraction pattern of *any* substance forming a single generalised lattice depend principally on the nature of the $Z(\mathbf{b})$-function.

Also, the distance statistics $z(\mathbf{x})$ of the generalised lattice whose Fourier transform is $Z(\mathbf{b})$ is then given by

$$z(\mathbf{x}) = \sum_{p_1=-\infty}^{\infty}\sum_{p_2=-\infty}^{\infty}\sum_{p_3=-\infty}^{\infty} H_{p_1p_2p_3}(\mathbf{x}) \tag{9}$$

$H_{p_1p_2p_3}(\mathbf{x})$ denotes the normalized distribution function for the location of the pth cell whose mean position is given by

$$\bar{\mathbf{x}}_p = p_1\bar{\mathbf{a}}_1 + p_2\bar{\mathbf{a}}_2 + p_3\bar{\mathbf{a}}_3 \tag{10}$$

p_k's are integers and $\bar{\mathbf{a}}_k$'s are the average values of the three fundamental lattice vectors.

III THE NEIGHBOUR STATISTICS AND RDF

In the case of "primitive" liquids, i.e., liquids containing no clusters, only one spherically symmetric coordination statistics, namely, the statistics of the first neighbour $H_1(r)$, is enough to locate the position of the pth neighbour.

It is given by (cf. Ref. 2),

$$H_1(r) = \frac{1}{(\pi\alpha^2)^{3/2}} \exp\left[-\frac{r^2}{\alpha^2}\right] \tag{11}$$

The statistics of the distribution of the pth neighbour $H_p(r)$ is consequently given by

$$H_p(r) = \frac{1}{4\pi^{3/2}m^{1/2}\alpha \cdot r_p} \frac{1}{r} \left\{ \exp\left[-\frac{(r - r_p)^2}{m\alpha^2}\right] - \exp\left[-\frac{(r + r_p)^2}{m\alpha^2}\right] \right\} \tag{12}$$

Here r_p denotes the distance of the centroid of the pth atom and m the number of convolutions by which it is reached from the origin with the help of $H_1(r)$. The probability of the distribution of the nth neighbours is thus

$$H_n(r) = 4\pi r^2 g(r) = \sum_p H_p(r) \tag{13}$$

$$g(r) = \overline{z(\mathbf{x}) - \delta(\mathbf{x} = 0)} \tag{13a}$$

The summation is to be taken over all the atoms belonging to the given nth neighbour. It is determined by the coordination number C_n; $\alpha^2/2 = \Delta^2 r$ denotes the mean-square fluctuation in any direction of the first neighbour statistics. It is evidently a measure of the dispersion of the distribution function.

It might be noted that neither $H_p(r)$ nor $H_n(r)$ are Gaussian functions and the properties of $H_n(r)$, i.e. of $g(r)$, is obtained by the convolution products of $H_1(r)$. Hence in order to obtain the (space-time averaged) distribution of atoms one must deconvolute the given $g(r)$-function. Consequently, it is obvious that the conventional method of analysis of RDF by putting Gaussian functions at the humps of the $g(r)$-function is neither mathematically nor physically correct.

For densely packed micro-clusters $g(r)$-function, being the convolution square of the density function, would not differ significantly from that of a homogeneous structure. Consequently, it can be analysed with sufficient accuracy with the help of a single function $H_1(r)$ to give reliable structural parameters. Actual inhomogeneities (at the atomic level) are revealed by those properties like pressure and compressibility which are very sensitive to the presence of clusters.

The presence of clusters can also be taken into account in the present methodology. For this, we have to introduce the distribution function $P_1(r)$ of the macro-lattice in which each of the clusters forms the building block, the "cell-element", of the macro-lattice.

It is interesting to note here that recently Baer[10] obtained an expression for $g(r)$ similar to Eq. (13) from considerations of "structural diffusion" of a locally fluctuating lattice and using Fokker–Planck equation. This concept of locally fluctuating lattice is very similar to that of generalised lattice, but not adequate enough to describe even an arbitrary homogeneous structure. A disordered lattice, from the point of view of dynamics, arises from anharmonic thermal vibrations of the perfectly crystalline lattice. It is known that anharmonic vibrations displace the equilibrium positions of atoms which in its turn can break up the lattice and can create holes in crystal lattice. Eventually, for large amplitudes of vibrations it gives rise to the liquid and to the amorphous state of the substance. Diffusion process is also really a result of the thermal motion. Unified Theory has taken account of all these factors which give rise to a generalised (distorted) lattice. From the standpoint of diffraction phenomena, unified theory shows that the three states (crystal, liquid and gas) of a substance can be looked upon as that of single generalised lattice structure. Holes are nothing but scatterers whose density is zero. Even a perfectly crystalline structure containing holes would give rise to the background scattering just as in the case of *perfect* mixed crystal. Therefore, for convenience of interpreting the diffraction diagrams in the unified theory two types of distortion were introduced. Distortion of the first kind is produced by thermal vibrations, holes, mixture of different types of atoms, etc., in otherwise a *perfect* lattice. The positions of the lattice points are not affected by such distortions. Distortion of the second kind describes the fluctuations of the lattice points themselves. Both can be handled independently and necessay criteria to determine these two types of distortions had been formulated before (see Refs. 1, 2). The $g(r)$-function contains both these two kinds of distortions and to determine the structural parameters we have to separate these two effects, both of them being the final result of anharmonic vibration. Further, it must be noted carefully that in the generalised lattice, the lattice vectors themselves do not vary independently in the general case. Consequently, locally fluctuating lattice as defined by Baer cannot produce an arbitrarily distorted lattice. Moreover, it must not be forgotten that the same distribution function can describe the density distribution of any substance (including "frozen" structures), which can be characterised as crystals, liquids or amorphous matter, at least so far as their diffraction patterns are concerned, depending on the value of α, i.e. the degree of disorder. Disordered structures may arise from a variety of causes and in most structures it is not the diffusion process which causes this disorder. Also the principal factor which creates the disorder of the liquid state (at least near the melting point), is not the diffusion process but large anharmonic lattice vibrations of the crystals. Consequently, Baer's method of derivation of the distribution function Eq. (12) cannot be relevant for the distribution function characterising a generalised lattice for all possible cases. Nevertheless, it is reassuring to find that the dynamic diffusion process also gives rise to a neighbour statistics like Eqs. (11) and (12).

IV ANALYSIS OF RDF AND EVALUATION OF THE STRUCTURAL PARAMETERS

From Eqs. (11), (12) and (13) it would seem that if we can determine $H_1(r)$, i.e. α by trial and error we would be able to obtain all the relevant information required to analyse the RDF curves of primitive liquids. The positions of r_p and C_n would be given by the corresponding crystal structure. But even simple liquids are not primitive liquids due to presence of holes and fissures, permitting diffusion process to occur, and the formation of aggregates of micro-cluster of distorted crystallites (for the evidences see Ref. 3). Consequently, in actual practice, if we do not introduce the distribution function of macro-lattice $P_1(r)$ and use only $H_1(r)$, we have to vary *simultaneously* (starting from the corresponding crystal structure), all the parameters α, r_p, C_n to get an accurate fit. One must try to fit the curves throughout the domain and not merely in the region of one or two humps of the $g(r)$-function. We have therefore used the method of least squares to fit the theoretical curve with the experimental one. The departure at the tail of the theoretical curve is due to the fact that for practical reasons only a few neighbours were taken for the calculation. Even then sometimes, as in Argon I and II, the first two peaks did not agree very well. The introduction of intercluster distance function $P_1(r)$ improved the fit considerably.†

One might think that since we have so many parameters to vary it is not unexpected that surprisingly good agreement as shown in the curves would be obtained. But it must be remembered that we are varying the parameters of the given crystal structure. A little trial would convince any sceptic that there is not much freedom in our choice. Consequently, it may be asserted that the parameters given in the relevant tables of this series of papers really represent the essential features of the liquid state quite adequately and satisfactorily.

(i) The methodology

Equation (1) shows that the function $g(r)$ contains the smearing effects of the distortion of the lattice as well as that of random thermal motions. Both these effects determine the interaction zone of the $g(r)$-function, that means, the distance at which it reaches its constant value $\bar{\rho}$. It is determined by $\Delta^2 r$ of the function $H_1(r)$. We have therefore to obtain from this the dispersion $\Delta^2 a$ due to the lattice distortion and the dispersion $\Delta^2 s$ due to harmonic thermal vibrations separately.

---

† For simple dense liquids it has been estimated that the average nearest neighbour distance within a cluster is approximately 0.8 to 0.9 Å shorter than the nearest neighbour of two adjacent clusters.

In general, the function $z(\mathbf{x})$ reaches its constant value where the neighbouring statistics along the direction $\mathbf{a}_k$ is so smeared out that its width in this direction of the lattice vector is equal to the average value of $\mathbf{a}_k$. In our case the distorted lattice would extend up to the pth neighbour if

$$p_l = \left(\frac{r_1}{\Delta a}\right)^2 \tag{14}$$

The linear dimension of the lattice is then given by

$$L = 2d \text{ Å} \tag{15}$$

where $|p_l| = d$ Å determines the interaction zone of the lattice. It should be noted that the distance of the nth neighbour $d_n \neq nr_1$, (r_1 denotes the nearest neighbour distance), but depends on the structure. The $g(r)$-function, however, does not give *directly* p_l but only the domain determined by the radial distance at which it reaches its constant value. This is due to the background scattering caused by thermal vibrations, different types of atoms as well as by the $Z(\mathbf{b})$-function. The humps of the $g(r)$-function therefore cease to be detected at $p_c{}^{\text{th}}$, ($p_c < p_l$), neighbour such that

$$p_c \approx \varepsilon^2 \left(\frac{r_1}{\Delta r}\right)^2 \tag{16}$$

where ε defines the so-called limiting ellipsoid of reflection at which humps of reflections could not be distinguished clearly from the background intensity. Detailed quantative analysis of the $Z(\mathbf{b})$-function had shown that if we assume that in order to distinguish a reflection the ratio of the maximum to the minimum of the reflection hump must attain at least a value $1 \cdot 1$, then $\varepsilon = 0.43$ (see Refs. 1, 2). As was discussed in the Ref. 3, this value of ε quite satisfactorily determined the observed numbers of reflections in the scattered intensity diagrams of liquids.

From Eq. (16) we see that p_c and the corresponding linear dimension of the interaction zone L_c of the $g(r)$-function can be easily calculated from $H_1(r)$. But in order to determine p_l (i.e. L), of Eqs. (14) and (15) we must calculate the distortion of the lattice positions themselves by separating out the effects of thermal vibrations around the mean position of the lattice. This is easily achieved by noting the relation (17)

$$H_1(r - r_1) = H_l(r - r_1) * H_{\text{th}}(r) \tag{17}$$

where $H_l(r - r_1)$ denotes the normalized distribution function for the neighbouring lattice whose most probable value is given by r_1 and $H_{\text{th}}(r)$ that due to harmonic thermal vibrations around each atom. From Eq. (17) it follows

$$\Delta^2 a = \Delta^2 r - \Delta^2 s \tag{18}$$

$\Delta^2 a$, $\Delta^2 s$ are the corresponding mean square fluctuations of H_l and H_{th}. $\Delta^2 s$ is calculated from Debye's theory of specific heat (for details, see Ref. 3).

Hence all the relevant significant structural parameters reported in the tables can be calculated from the proper analysis of the experimentally obtained $g(r)$-function with the help of the unified kinematic theory of diffraction.

V RESULTS

The RDF of argon at various temperatures and pressures obtained by Eisenstein and Gringrich[11] have been numbered according to these authors. The particulars of the samples are noted in Table I. The data for Gringrich I, II and IV were taken from Schmidt and Tompson.[12] Others were taken from the published graphs by Eisenstein and Gingrich. Only the sample number VII is vapour. Others are liquids. All the samples were investigated near the saturated vapour curve.

TABLE I

Temperature, pressure and density of Eisenstein and Gingrich argon

	T (°K)	P (Atm)	ρ (gm/cc)
I	84.25	0.8	1.401
II	91.8	1.8	1.365
IV	126.7	18.3	1.10
V	144.1	37.7	0.87
VI	149.3	46.8	0.737
VII	149.3	43.8	0.330

Table II gives the relevant structure parameters, and Table III the distances r_n of different neighbours and their coordination numbers C_n as well as the values of m, the number of convolutions. Figures 1, 2 and 3 show the experimental values (+) and calculated values (−) as well as the distance statistics of the various neighbours.

Argon I and argon II were also reported in the paper by Bagchi,[3] but the fit (particularly for the first two neighbours) was not very good. It was concluded that this was due to the presence of clusters. By incorporating the first inter-cluster neighbour statistics the agreement became very satisfactory. It is interesting to note that all liquid argon shows clustering effects, but its vapour doesn't.

For comparison, recent data on liquid argon at 84°K by neutron diffraction reported by Yarnell *et al.*[13] has also been analysed and is incorporated

TABLE II

Structural parameters for Gingrich and Yarnell Argon

	Gingrich I	Gingrich II	Gingrich IV	Gingrich V	Gingrich VI	Gingrich VII	Yarnell
T (°K)	84.25	91.80	126.7	144.1	149.3	149.3	85.00
θ (°K)	80	80	80	80	80	80	80
α	0.5478	0.4322	0.5254	0.5538	0.9998	0.8393	0.5777
r_1	3.808	3.734	3.719	3.996	4.008	4.026	3.821
$\Delta^2 r$	0.1500	0.0934	0.1380	0.1533	0.4998	0.3522	0.1668
$\Delta r/r_1$ %	10.17	8.186	9.990	9.799	17.64	14.74	10.69
$\|p_c\|$	24	37	25	26	8	12	22
L_c (A^0)	18.66	22.71	18.59	20.38	11.34	13.95	17.92
$\Delta^2 s$	0.04884	0.05301	0.07242	0.08216	0.08507	0.08507	0.04925
$\Delta^2 a$	0.1012	0.04039	0.06559	0.07117	0.4147	0.2672	0.1176
$\Delta a/r_1$ %	8.354	5.383	6.887	6.676	16.07	12.84	8.975
$\|p_l\|$	143	345	211	224	39	61	124
L(Å)	91.07	138.7	108.0	119.6	50.07	62.90	85.10

TABLE III

Neighbour statistic for Gingrich and Yarnell Argon

	Gingrich I	Gingrich II	Gingrich IV	Gingrich V	Gingrich VI	Gingrich VII	Yarnell
Σ^2	26.985	2.8760	3.2487	2.4031	0.36325	0.07325	50.658
α	0.54777	0.43221	0.52538	0.55376	0.99979	0.83932	0.57766
m	r / C	r / C	r / C	r / C	r / C	r / C	r / C
1	3.808/ 10.21	3.734/ 6.621	3.719/ 4.567	3.996/ 4.017	4.008/ 2.912	4.026/ 2.083	3.821/ 9.903
2	4.729 3.243						4.873 3.471
2	5.979 9.048	4.622 6.109	4.623 5.781	4.908 3.378	4.765 3.370	5.387 1.641	6.084 8.901
2	7.123 20.77	5.924 8.689	6.001 8.076	5.895 5.439	5.781 4.117	6.205 2.520	7.111 20.64
2	8.134 13.37	6.898 12.50	7.128 12.80	7.146 9.450	7.546 7.544	7.846 3.303	8.137 13.29
3	9.369 24.73	7.872 20.48	8.550 26.28	8.547 20.14	8.282 15.98	8.039 4.821	9.431 24.81
3	9.380 7.989						9.432 8.070
3	10.71 44.03						10.69 43.90
4	12.02 8.393						12.09 8.407
3	12.02 13.74						12.09 13.76
4	12.27 24.51						12.35 24.49
4	12.70 24.28						12.68 24.27
4	13.51 23.62						13.75 23.62

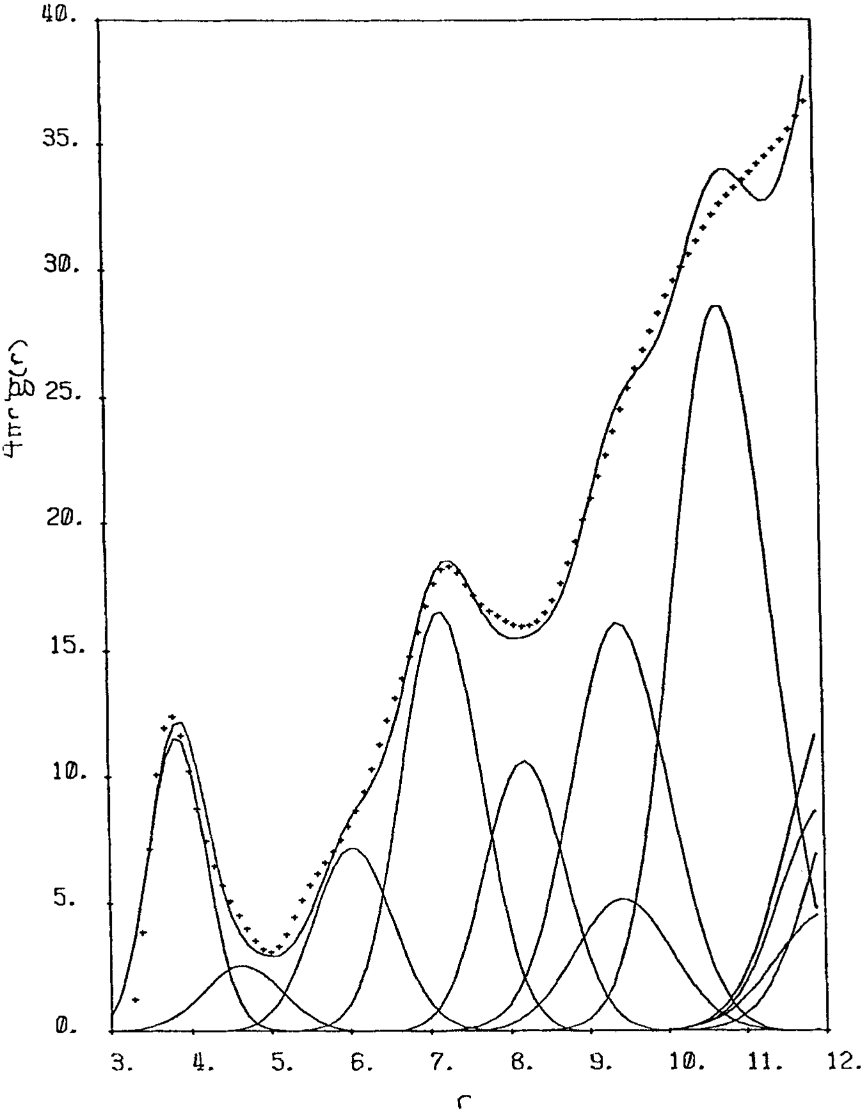

FIGURE 1 Gingrich Argon I with cluster. Experimental (+ + +) and calculated (———) RDF by varying all parameters simultaneously. Neighbours (———) are also shown.

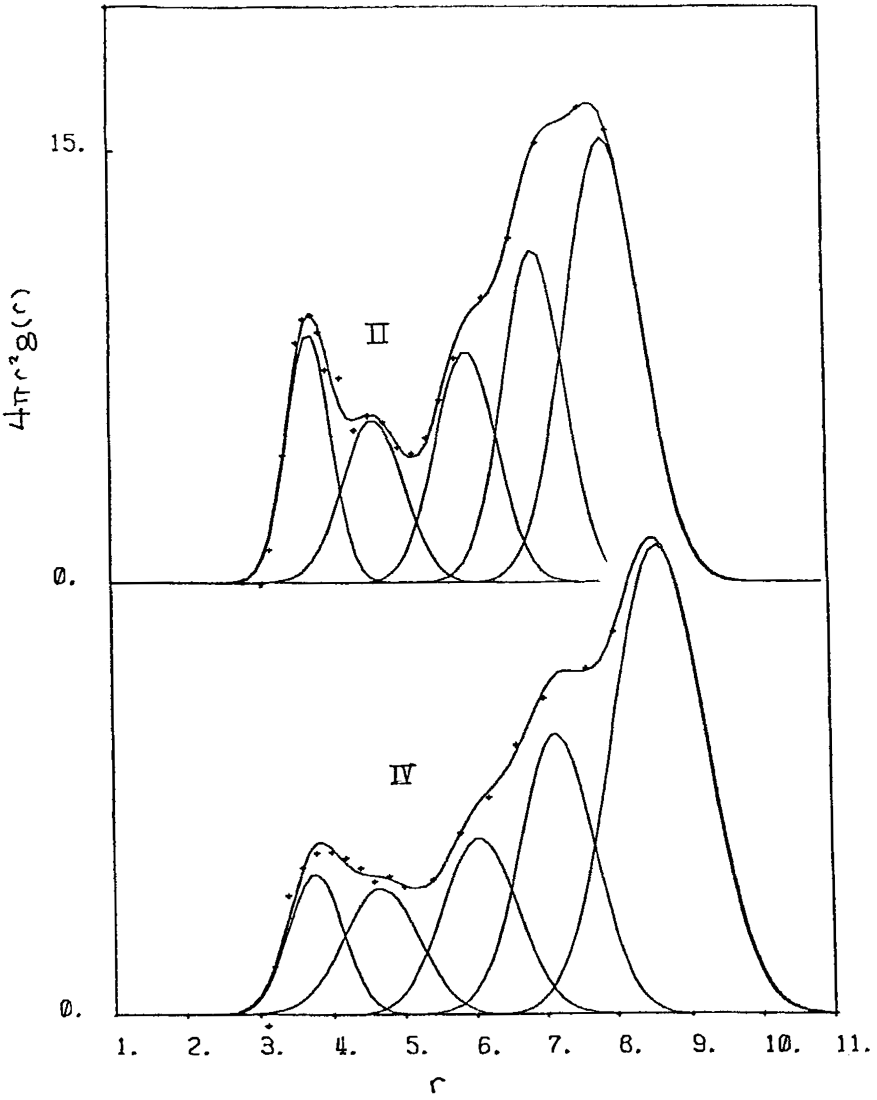

FIGURE 2 Gingrich Argon II and IV. Experimental (+ + +) and calculated (———) RDF by varying all parameters simultaneously. Neighbours (———) are also shown. Vertical scale is shifted 15 units.

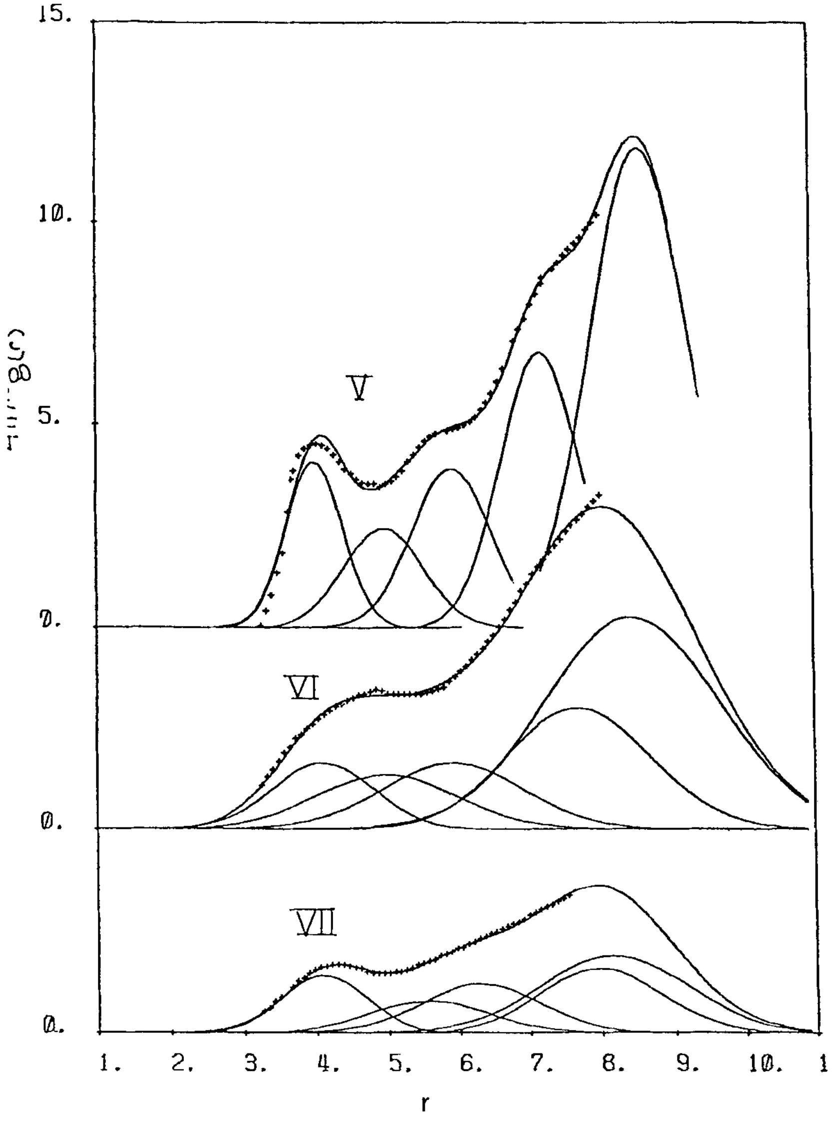

FIGURE 3 Gingrich Argon V, VI and VII. Experimental (+ + +) and calculated (———) RDF by varying all parameters simultaneously. Neighbours (———) are also shown. Vertical scale successively shifted by 5 units.

in Table II. As in the case of the neutron diffraction data by Henshaw[14] reported by Bagchi,[3] we find here also that neutrons agitate the atoms more violently but the overall effect remains practically the same.

As expected, the density affects significantly only the coordination numbers. The effects of pressure and temperature separately could not be studied quantitatively due to lack of systematic data. Such systematic data would be useful for deriving the equations of state of the liquid.

We also analysed the X-ray diffraction data for the 13 samples of argon near the critical region given by Mikolaj and Pings (see Ref. 12). The samples are described in Table IV.

TABLE IV

Temperature, pressure and density for Pings Argon

Sample	T (°K)	ρ (gm/cc)	P (Atm)
1	143	0.910	39.32
2	143	0.982	65.63
3	148	0.280	42.51
4	148	0.780	44.11
5	148	0.910	65.70
6	148	0.982	97.89
7	153	0.536	52.72
8	153	0.780	61.76
9	153	0.910	91.89
10	158	0.536	62.31
11	163	0.280	55.52
12	163	0.536	72.01
13	163	0.780	98.39

Table V gives the structure parameters of all 13 curves and Table VI the distances of neighbours and coordination numbers. The sum of squares $\sum^2$ is also noted.

Figures 4, 5, 6 and 7 show the calculated and experimental curves of RDF as well as neighbour statistics. In order to avoid clumsiness, only one neighbour statistics belonging to the lowest curve is shown in some cases.

It is interesting to note that contrary to the liquid argon reported by Gingrich, all the curves of liquid argon reported by Mikolaj and Pings seem to be statistically homogeneous on the atomic scale.

The interaction zone of the $g(r)$-function decreases with temperature as expected from the observed diffraction patterns. The fluctuation of the neighbour statistics generally increases with the rise of temperature; but nevertheless remains finite, with about 10%–15% usually found for all the liquid states.

TABLE V

Structural parameters for Pings Argon

	Pings 1	Pings 2	Pings 3	Pings 4	Pings 5	Pings 6	Pings 7
T (°K)	143.0	143.0	148.0	148.0	148.0	148.0	153.0
θ (°K)	80	80	80	80	80	80	80
α	0.7346	0.6709	0.6123	0.7454	0.7362	0.6576	0.7016
r_1	3.913	3.901	3.884	3.909	3.883	3.867	3.920
$\Delta^2 r$	0.2698	0.2251	0.1875	0.2778	0.2710	0.2162	0.2461
$\Delta r/r_1$ %	13.28	12.16	11.15	13.49	13.41	12.03	12.66
$\lvert p_c \rvert$	14	17	20	14	14	17	16
L_c (Å)	14.64	16.08	17.37	14.63	14.53	15.94	15.68
$\Delta^2 s$	0.08154	0.08154	0.08434	0.08434	0.08434	0.08434	0.08715
$\Delta^2 a$	0.1883	0.1435	0.1031	0.1935	0.1866	0.1319	0.1590
$\Delta \mathrm{a}/r_1$ %	11.09	9.713	8.268	11.25	11.13	9.392	10.17
$\lvert p_l \rvert$	81	106	146	79	81	113	97
L (Å)	70.43	80.32	93.86	69.48	69.89	82.21	77.21

	Pings 8	Pings 9	Pings 10	Pings 11	Pings 12	Pings 13
T °K)	153.0	153.0	158.0	163.0	163.0	163.0
θ (°K)	80	80	80	80	80	80
α	0.7480	0.6949	0.6689	0.6394	0.6798	0.7171
r_1	3.910	3.902	3.879	3.898	3.965	3.932
$\Delta^2 r$	0.2798	0.2415	0.2237	0.2044	0.2311	0.2571
$\Delta r/r_1$%	13.53	12.59	12.19	11.60	12.12	12.90
$\lvert p_c \rvert$	14	16	17	19	17	15
L_c(Å)	14.63	15.61	15.99	16.99	16.35	15.23
$\Delta^2 s$	0.08715	0.08715	0.08995	0.09275	0.09275	0.09275
$\Delta^2 a$	0.1926	0.1543	0.1338	0.1117	0.1383	0.1643
$\Delta a/r_1$ %	11.23	10.07	9.430	8.574	9.380	10.31
$\lvert p_l \rvert$	79	99	112	136	114	94
L(Å)	69.50	77.65	82.11	90.90	84.67	76.24

TABLE VI

Neighbour statistics for Pings Argon

	Pings 1	Pings 2	Pings 3	Pings 4	Pings 5	Pings 6	Pings 7
Σ^2	2.6979	1.8447	0.32818	2.5036	3.4272	3.3257	0.70067
α	0.73459	0.67094	0.61234	0.74544	0.73619	0.65764	0.70162
m	*r* / *C*	*r* / *C*	*r* / *C*	*r* / *C*	*r* / *C*	*r* / *C*	*r* / *C*
1	3.913/ 5.479	3.901/ 5.718	3.844/ 1.756	3.909/ 5.002	3.883/ 5.478	3.867/ 5.894	3.920/ 3.475
2	5.204 5.703	5.194 5.982	5.090 2.102	5.227 5.028	5.214 5.699	5.154 6.024	5.223 3.785
2	6.489 6.946	6.476 7.288	6.424 2.789	6.528 6.244	6.495 6.951	6.471 7.344	6.493 4.609
2	7.424 7.850	7.366 8.259	7.485 2.918	7.433 7.061	7.409 7.853	7.336 8.288	7.452 4.949
3	8.306 14.69	8.266 15.38	8.589 5.158	8.425 13.30	8.305 14.69	8.266 15.42	8.478 9.733
3	9.066 3.261	8.988 3.417	9.023 1.229	9.082 2.977	9.066 3.260	8.974 3.422	9.041 2.198
3	9.830 19.10	9.725 19.95	10.06 6.574	9.935 17.48	9.828 19.09	9.724 19.94	10.01 12.71
4	10.51 3.579	10.53 3.727	10.56 1.264	10.56 3.307	10.51 3.578	10.54 3.733	10.62 2.331
3	11.16 8.043	11.10 8.318	11.22 2.600	11.29 7.476	11.16 8.043	11.11 8.349	11.43 4.995
4	11.16 14.65	11.09 15.13	11.55 4.762	11.41 13.65	11.16 14.65	11.10 15.18	11.51 9.052
4	11.69 10.98	11.47 11.28	12.08 3.606	11.90 10.36	11.69 10.98	11.46 11.30	11.83 6.751
4	12.26 8.219	12.06 8.403	12.40 2.962	12.43 7.869	12.26 8.218	12.04 8.408	12.31 5.297
4	12.83 8.491	12.71 8.635	12.80 3.798	13.00 8.240	12.84 8.491	12.70 8.634	12.94 6.091
5	13.35 11.78	13.17 11.92	13.52 6.987	13.50 11.53	13.35 11.78	13.17 11.92	13.51 9.425
4	13.37 22.54	13.24 22.81	14.60 16.46	13.83 22.11	13.37 22.54	13.25 22.81	14.03 19.25

TABLE VI (*continued*)

	Pings 8	Pings 9	Pings 10	Pings11	Pings 12	Pings 13
Σ^2	2.6363	2.1157	0.76774	0.14046	0.36144	1.3278
α	0.74801	0.69493	0.66895	0.63940	0.67982	0.71707
m	r / C	r / C	r / C	r / C	r / C	r / C
1	3.910/ 5.029	3.902/ 5.571	3.879/ 3.354	3.898/ 1.670	3.965/ 3.434	3.932/ 5.028
2	5.210 5.032	5.199 5.661	5.190 3.714	5.106 2.005	5.254 3.703	5.257 5.000
2	6.536 6.201	6.496 6.961	6.483 4.583	6.424 2.700	6.516 4.537	6.531 6.202
2	7.450 7.047	7.388 7.848	7.438 4.887	7.512 2.803	7.479 4.868	7.448 7.030
3	8.435 13.29	8.330 14.69	8.502 9.711	8.607 4.991	8.531 9.623	8.461 13.27
3	9.081 2.970	9.020 3.261	9.033 2.194	9.053 1.190	9.033 2.174	9.077 2.968
3	9.967 17.48	9.816 19.07	10.01 12.53	10.04 6.466	10.02 12.60	9.950 17.45
4	10.56 3.302	10.55 3.580	10.60 2.319	10.56 1.247	10.62 2.306	10.57 3.299
3	11.30 7.468	11.19 8.054	11.41 5.018	11.28 2.580	11.43 4.949	11.33 7.465
4	11.43 13.64	11.20 14.66	11.52 9.095	11.56 4.722	11.54 8.977	11.45 13.64
4	11.92 10.35	11.63 10.98	11.88 6.788	12.03 3.568	11.87 6.702	11.91 10.35
4	12.44 7.865	12.19 8.215	12.35 5.307	12.37 2.924	12.34 5.271	12.42 7.864
4	13.01 8.239	12.80 8.483	12.94 6.072	12.83 3.759	12.96 6.078	13.00 8.237
5	13.51 11.53	13.55 11.77	13.51 9.389	13.59 6.969	13.53 9.414	13.50 11.52
4	13.84 22.11	13.39 22.52	14.04 19.17	14.61 16.48	14.06 19.24	13.85 22.11

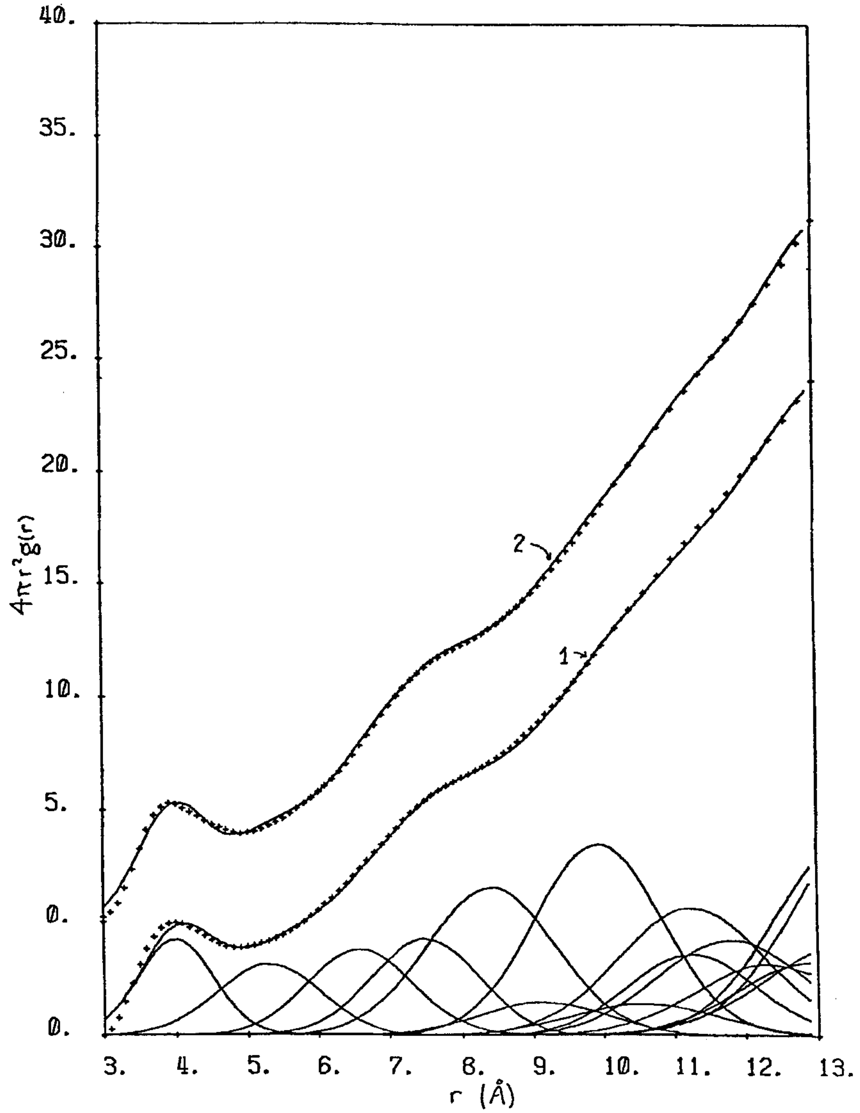

FIGURE 4 Mikolaj and Pings Argon 1 and 2. Experimental (+ + +) and calculated (———) RDF by varying all parameters simultaneously. Neighbours (———) are also shown for 1. Vertical scale is shifted by 5 units.

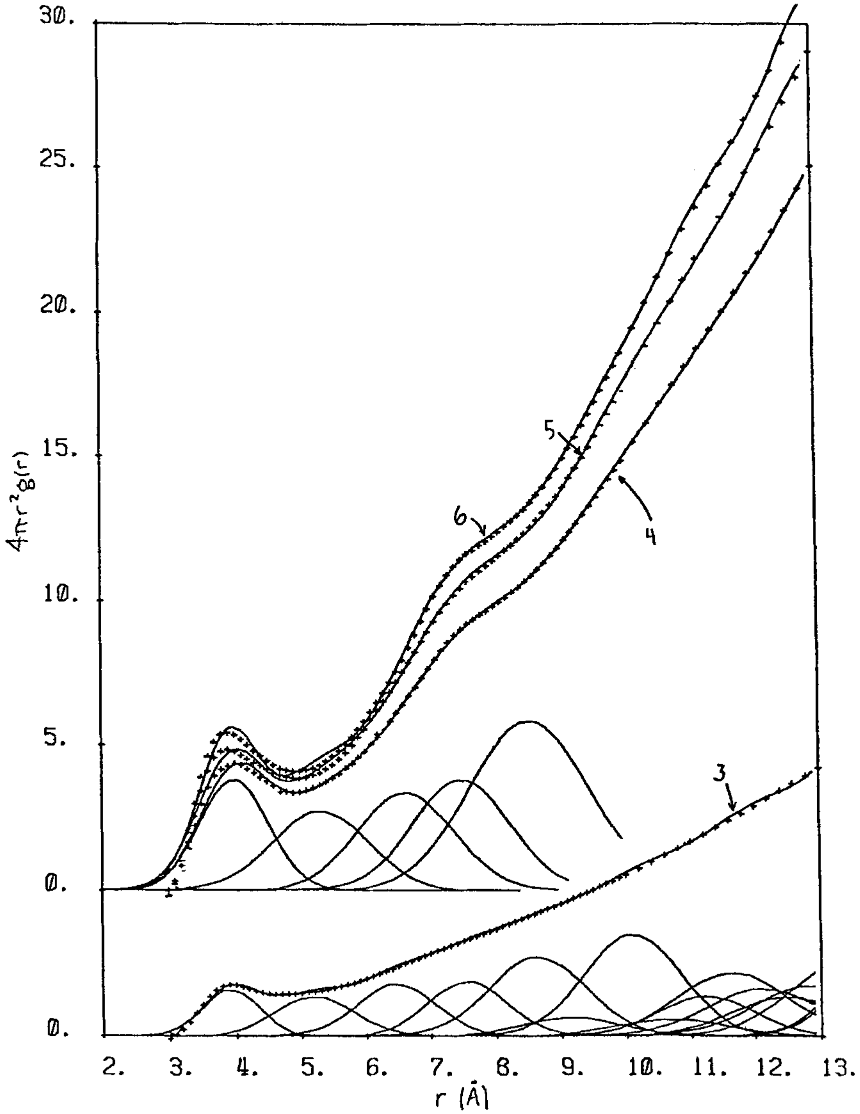

FIGURE 5 Mikolaj and Pings Argon 3, 4, 5 and 6. Experimental (+ + +) and calculated (———) RDF by varying all parameters simultaneously. Neighbours (———) are also shown for 3 and 4. Vertical scale shifted by 5 units.

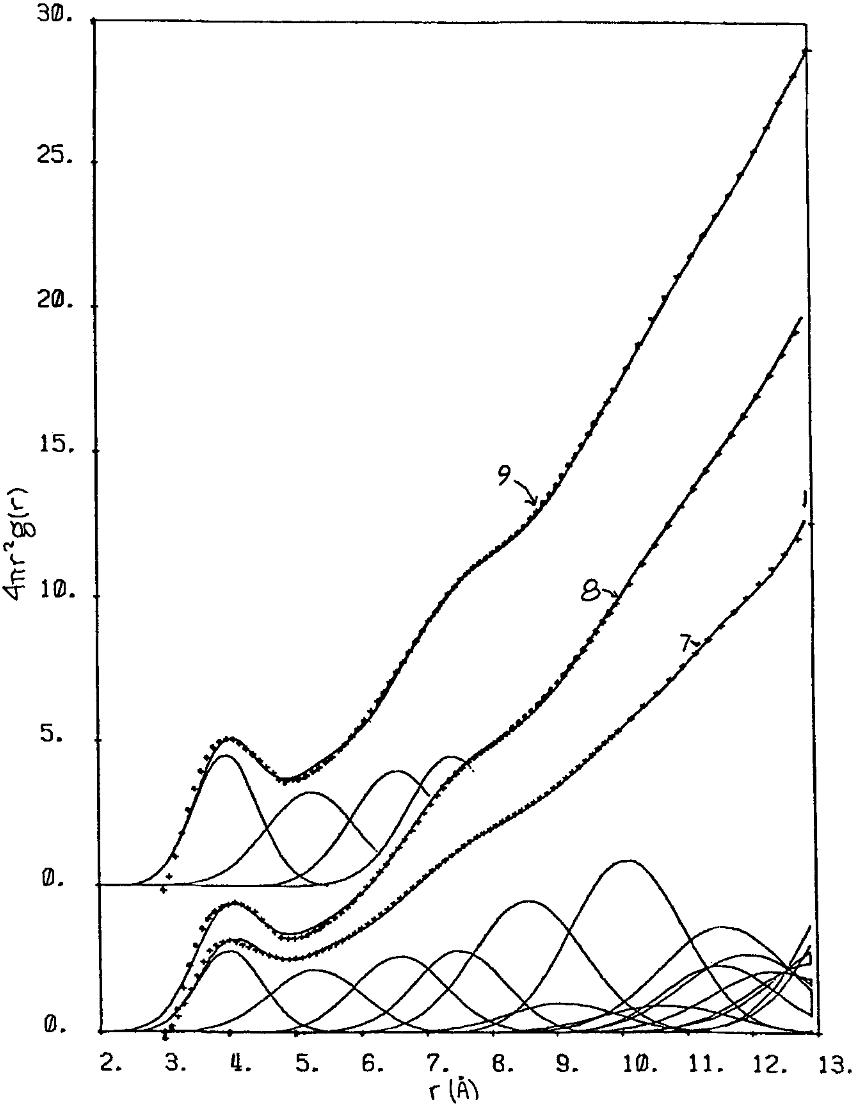

FIGURE 6 Mikolaj and Pings Argon 7, 8 and 9. Experimental (+ + +) and calculated (———) RDF by varying all parameters simultaneously. Neighbours (———) are also shown for 7 and 9. Vertical scale is shifted by 5 units.

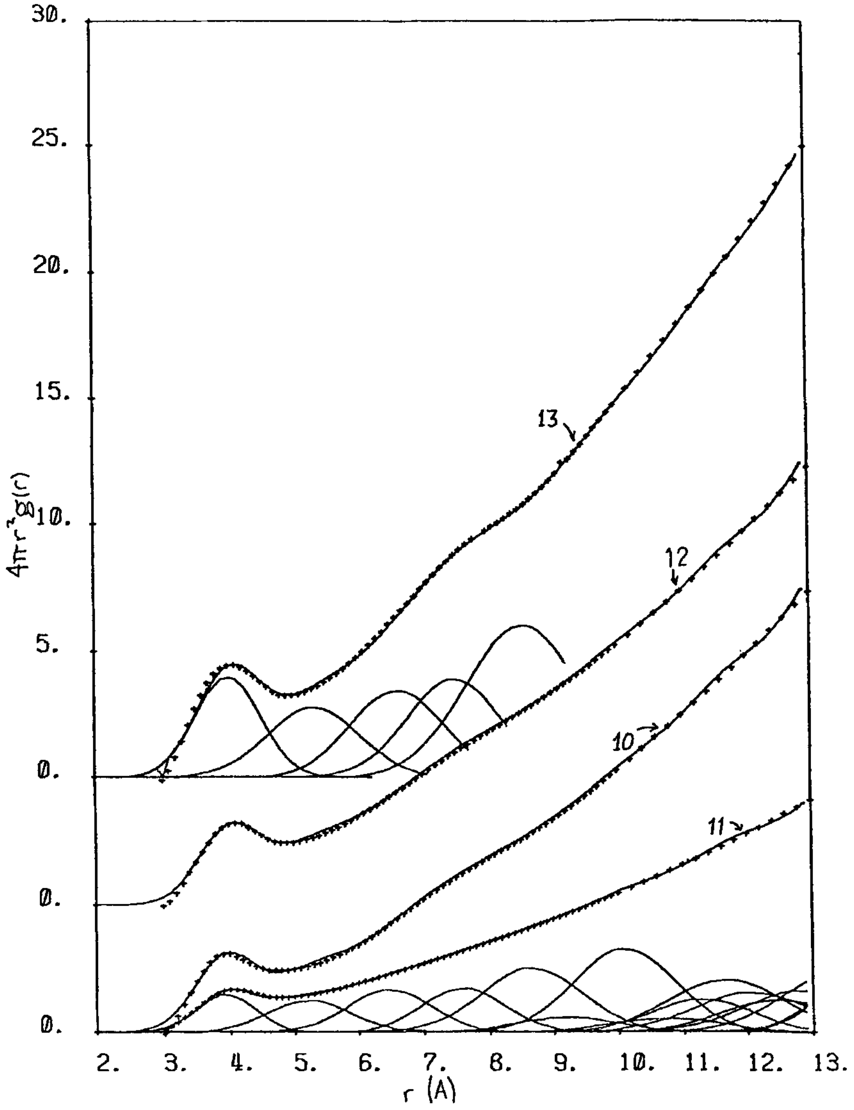

FIGURE 7 Mikolaj and Pings Argon 10, 11, 12 and 13. Experimental (+ + +) and calculated (———) RDF by varying all parameters simultaneously. Neighbours (———) are also shown for 11 and 13. Vertical scales are shifted by 5 units.

References

1. R. Hosemann and S. N. Bagchi, *Direct Analysis of Diffraction by Matter*, North Holland, Amsterdam (1962).
2. S. N. Bagchi, *Adv. Phys.*, **19**, 119 (1970).
3. S. N. Bagchi, *Acta Cryst.*, **A28**, 560 (1972).
4. S. N. Bagchi and J. P. Supple, *Phys. Chem.Liq.*, **8**, 223 (1979).
5. F. Zernike and J. A. Prins, *Z. Phys.*, **41**, 184 (1927).
6. R. Hosemann and S. N. Bagchi, *Acta Cryst.*, **5**, 749 (1952).
7. R. Hosemann and S. N. Bagchi, *Acta Cryst.*, **6**, 318 (1953).
8. R. Hosemann and S. N. Bagchi, *Acta Cryst.*, **6**, 404 (1953).
9. S. N. Bagchi (1973) Symposial Papers, Vol IV (11), p. 775, of the Int. Biophysics Congress, Moscow (1972).
10. S. Baer, *Physica*, **91A**, 603 (1978).
11. A. Eisenstein and N. S. Gingrich, *Phys. Rev.*, **62**, 261 (1942).
12. P. W. Schmidt and C. W. Tompson, "X Ray scattering studies of simple fluids," *Simple Dense Fluids*, Academic Press, New York (1968), ed., H. L. Frisch and Z. E. Salsburg.
13. J. L. Yarnell, M. J. Katz, and R. G. Wenzel, *Phys. Rev.*, **A7**, 2130 (1973).
14. D. G. Henshaw, *Phys. Rev.*, **105**, 976 (1957).